

## RESEARCH ARTICLE Winter Water Properties and the Chukchi Polynya

10.1002/2016JC011918

C. Ladd<sup>1</sup>, C. W. Mordy<sup>1,2</sup>, S. A. Salo<sup>1</sup>, and P. J. Stabeno<sup>1</sup>

## Key Points:

- Upwelled Atlantic Water is observed on the Chukchi Shelf, far from Barrow Canyon
- Atlantic Water is often associated with the Chukchi Polynya
- Chukchi Polynya can often be classified as a hybrid sensible heat/wind-driven polynya

## Correspondence to:

C. Ladd,  
carol.ladd@noaa.gov

## Citation:

Ladd, C., C. W. Mordy, S. A. Salo, and P. J. Stabeno (2016), Winter Water Properties and the Chukchi Polynya, *J. Geophys. Res. Oceans*, 121, 5516–5534, doi:10.1002/2016JC011918.

Received 26 APR 2016

Accepted 8 JUL 2016

Accepted article online 13 JUL 2016

Published online 5 AUG 2016

<sup>1</sup>Pacific Marine Environmental Laboratory, NOAA, Seattle, Washington, USA, <sup>2</sup>Joint Institute for the Study of the Atmosphere and Ocean, University of Washington, Seattle, Washington, USA

**Abstract** Water properties from moored measurements (2010–2015) near Icy Cape on the eastern Chukchi shelf have been examined in relation to satellite observations of ice cover. Atlantic Water (AW), with temperature  $> -1^{\circ}\text{C}$  and salinity  $> 33.6$ , has been observed to upwell from deeper than 200 m in the Arctic Basin onto the Chukchi Shelf via Barrow Canyon. Most previous observations of AW on the Chukchi shelf have been in or near Barrow Canyon; observations of AW farther onto the shelf are rare. Despite mooring location on the shelf  $\sim 225$  km from the head of Barrow Canyon, five AW events have been observed at mooring C1 ( $70.8^{\circ}\text{N}$ ,  $163.2^{\circ}\text{W}$ ) in 4 years of data. All but one of the events occurred under openings in the sea-ice cover (either a polynya or the ice edge). No events were observed during the winter of 2011/2012, a year with little polynya activity in the region. In addition to changes in temperature and salinity, the AW events are typically associated with southwestward winds and currents, changes in sea-ice cover, and increased nutrient concentrations in the bottom water. Estimates of heat content associated with the AW events suggest that the Chukchi Polynya can often be classified as a hybrid sensible heat/wind-driven polynya.

## 1. Introduction

### 1.1. Circulation

The Chukchi Sea is a broad, shallow arctic sea. During winter, the shelf is ice covered. Ice retreat begins in spring and by September, the shelf is largely ice-free. Pacific Waters flow northward through Bering Strait to the Chukchi Sea en route to the Arctic Basin. Northward transport through Bering Strait is seasonal, averaging 1.0 Sv ( $1 \text{ Sv} = 10^6 \text{ m}^3 \text{ s}^{-1}$ ) during April–September and 0.6 Sv during October–March [Woodgate *et al.*, 2005a], driven by the combination of a Pacific–Arctic pressure difference [Coachman and Aagaard, 1966; Coachman *et al.*, 1975], and local wind effects [Woodgate *et al.*, 2005b]. Northward transport across the Chukchi Sea shelf follows three main pathways influenced by the bathymetry of the shelf: flow through Herald Canyon [Coachman *et al.*, 1975; Pickart *et al.*, 2010; Weingartner *et al.*, 2005; Woodgate and Aagaard, 2005]; flow through the Central Channel between Herald and Hanna Shoals [Weingartner *et al.*, 2005]; and flow close to the Alaskan coast, exiting the shelf through Barrow Canyon [Coachman *et al.*, 1975] (Figure 1). Northward (down-canyon) flow in Barrow Canyon is strongest in summer and weaker in winter [Aagaard and Roach, 1990; Itoh *et al.*, 2013; Weingartner *et al.*, 2005, 1998] and is often interrupted by up-canyon flow of upwelled water onto the shelf. Upwelling in Barrow Canyon is most frequent in the fall [Aagaard and Roach, 1990].

### 1.2. Water Masses

In late summer, the Chukchi Sea exhibits a two-layer water column with well-mixed surface and bottom layers separated by a strong pycnocline. During winter (the focus of our study), surface cooling, wind mixing from storms, and brine rejection from ice formation vertically mix the water column. The various water masses of the Chukchi Sea have been described by numerous investigators [e.g., Coachman *et al.*, 1975; Danielson *et al.*, 2016; Gong and Pickart, 2015]. The warmest water in the eastern Chukchi Sea is Alaskan Coastal Water (ACW) which enters the Chukchi Sea via Bering Strait in mid to late summer. The coldest water mass, Pacific Winter Water (PWW), enters the Chukchi Sea through Bering Strait during winter and is modified in regions of ice formation where brine rejection acts to increase the salinity of PWW [Itoh *et al.*, 2012; Woodgate *et al.*, 2005a]. PWW flows off the shelf into the Arctic basin, sinking to feed the cold Arctic halocline which shields the surface mixed layer from the warmer, saltier Atlantic layer below [Aagaard *et al.*, 1981; Coachman *et al.*, 1975; Shimada *et al.*, 2005]. While various investigators use different definitions, Gong and Pickart [2015] define ACW as water with potential temperature  $> 3^{\circ}\text{C}$  and PWW as that colder than

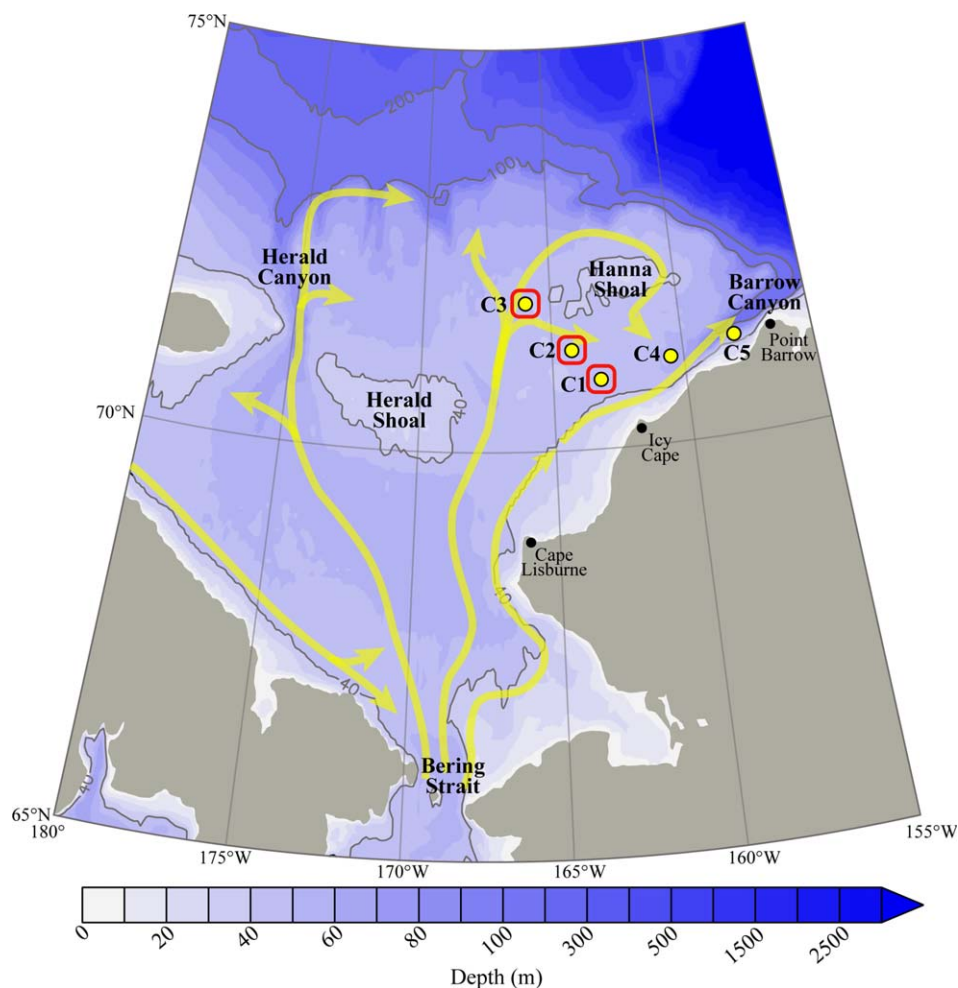


**Figure 1.** Map of the Chukchi Sea showing bathymetry (color scale; m) and schematic currents, location of moorings C1–C5 (yellow circles), location of regions used for calculating time series of percent ice cover from SSM/I (red squares).

$-1^{\circ}\text{C}$ . We will broadly distinguish between bottom waters influenced by warm ACW and cold PWW. Special attention will be paid to upwelled relatively warm and salty Atlantic Water (AW).

Upwelling events occur frequently in Barrow Canyon and the majority of these events result in reintroduction of PWW onto the shelf [Schulze and Pickart, 2012]. During some upwelling events, Atlantic Water (AW), with potential temperature  $> -1^{\circ}\text{C}$  and salinity  $> 33.6$ , has been observed to upwell from deeper than 200 m in the Arctic Basin onto the Chukchi Shelf via Barrow Canyon. Upwelling of AW has been attributed to easterly wind events [e.g., Pickart et al., 2009, 2011] and/or shelf waves [Aagaard and Roach, 1990] and the heat flux associated with the upwelling events has been found to be large enough to be of local significance to the surface heat budget [Aagaard and Roach, 1990; Hirano et al., 2016]. Easterly winds produce the strongest upwelling response during the partial ice season when mobile ice keels can result in enhanced surface stresses. While the response is weaker during full ice cover, upwelling events are still observed [Pickart et al., 2013; Schulze and Pickart, 2012; Williams et al., 2006]. Most observations of AW on the Chukchi shelf have been in or near Barrow Canyon [Aagaard and Roach, 1990; Garrison and Paquette, 1982; Itoh et al., 2013; Mountain et al., 1976]. However, Bourke and Paquette [1976] observed AW as far onto the shelf as Icy Cape ( $\sim 225$  km from the head of Barrow Canyon) in August 1975. They note similar occurrences of AW farther onto the shelf in 1922 and 1958 but suggest that such occurrences are rare.

### 1.3. Polynyas

The polynya that occurs along the Alaskan coast between Cape Lisburne and Point Barrow is the largest in the western Arctic [Itoh et al., 2012]. Ice formation and brine rejection in the polynya results in increased

**Table 1.** Mooring Depths, Locations, and Years Deployed

Mooring	Years Deployed	Latitude (°N)	Longitude (°W)	Depth (m)
C1	2010, 2011, 2013, 2014	70.84	163.20	46
C2	2010, 2011, 2012, 2013, 2014	71.22	164.25	44
C3	2010, 2011	71.83	165.98	45
C4	2012, 2013, 2014	71.04	160.49	44
C5	2013, 2014	71.21	158.00	45

salinity of the PWW to form the densest water mass to enter the western Arctic Ocean [Aagaard *et al.*, 1981; Weingartner *et al.*, 2005, 1998] resulting in a significant contribution to the cold halocline layer of the Arctic Ocean [Cavalieri and Martin, 1994]. The thick temperature minimum and cold halocline layer form an effective barrier between the relatively fresh surface mixed layer of the Arctic and the warmer, saltier Atlantic layer below [Shimada *et al.*, 2005].

Polynyas are traditionally defined by their formation and maintenance mechanism as either “sensible heat” or “wind-driven.” Sensible heat polynyas are a result of oceanic sensible heat melting (or preventing formation of) ice. Wind-driven polynyas (also referred to as “latent heat polynyas”) are mechanically driven via divergent ice motion due to winds or currents. In wind-driven polynyas, the water is usually at the freezing temperature and heat loss to the atmosphere results in high rates of ice formation [Morales Maqueda *et al.*, 2004]. Most shelf water polynyas are wind-driven polynyas but there are exceptions. Many polynyas in the Canadian Arctic Archipelago are caused by surfacing of warm Atlantic water due to tide-induced mixing (sensible heat polynyas) [Melling *et al.*, 1984]. In other cases, shelf water polynyas are maintained by both sensible heat and wind forcing [Kozo, 1991; Morales Maqueda *et al.*, 2004]. It has been largely assumed that the polynyas observed in the eastern Chukchi Sea are wind-driven polynyas formed through wind forced coastal divergence. However, mooring data over Barrow Canyon in 2009/2010 suggest that heat flux associated with upwelled AW plays a role in polynya formation there [Hirano *et al.*, 2016]. Hirano *et al.* [2016] suggest that the Barrow Coastal Polynya should be considered a wind-driven hybrid polynya, with both sensible heat and wind-driven divergence caused by the northeasterly wind.

## 2. Data and Methods

### 2.1. Mooring Data

A series of moorings has been deployed in the eastern Chukchi Sea since 2010 (Table 1). Moorings were deployed in August or September and recovered approximately 1 year later. Mooring designs were identical for each year. To avoid ice keels, each mooring was <10 m off the bottom. We report near-bottom temperature and salinity (Sea-Bird Scientific Seacat), nitrate (Satlantic ISUS), and currents (300 or 600 kHz Teledyne Sentinel Acoustic Doppler Current Profiler; ADCP). Data were collected at least hourly and all instruments were calibrated prior to deployment. The physical and chemical data were processed according to the manufacturers' specifications. All current time series were low-pass filtered with a 35 h, cosine-squared, tapered Lanczos filter to remove tidal and higher-frequency variability, and resampled at 6 h intervals. CTD and water bottle casts were conducted following or preceding mooring recoveries and deployments to provide quality control of the data collected by some of the instruments on the moorings (e.g., temperature, salinity, and nitrate). Vertical shears calculated from unfiltered ADCP velocities are used to examine likely periods of enhanced mixing.

### 2.2. Other Data

The NOAA/NSIDC Climate Data Record sea-ice concentrations [Meier *et al.*, 2013, updated 2015; Peng *et al.*, 2013] (downloaded from nsidc.org) are an estimate of the fraction of ocean area covered by sea ice. These data are produced by combining concentration estimates created using two algorithms developed at the NASA Goddard Space Flight Center (GSFC): the NASA Team algorithm [Cavalieri *et al.*, 1984] and the Bootstrap algorithm [Comiso, 1986]. NSIDC applies the individual algorithms to brightness temperature data from Remote Sensing Systems, Inc. (RSS). Sea-ice concentrations were averaged over three regions surrounding moorings C1–C3 (Figure 1) to obtain time series for the 5 years of our study. Maps of daily sea-ice concentration are shown for select periods of time and monthly climatologies were calculated using the five winters of our study period to examine the mean seasonal cycle.

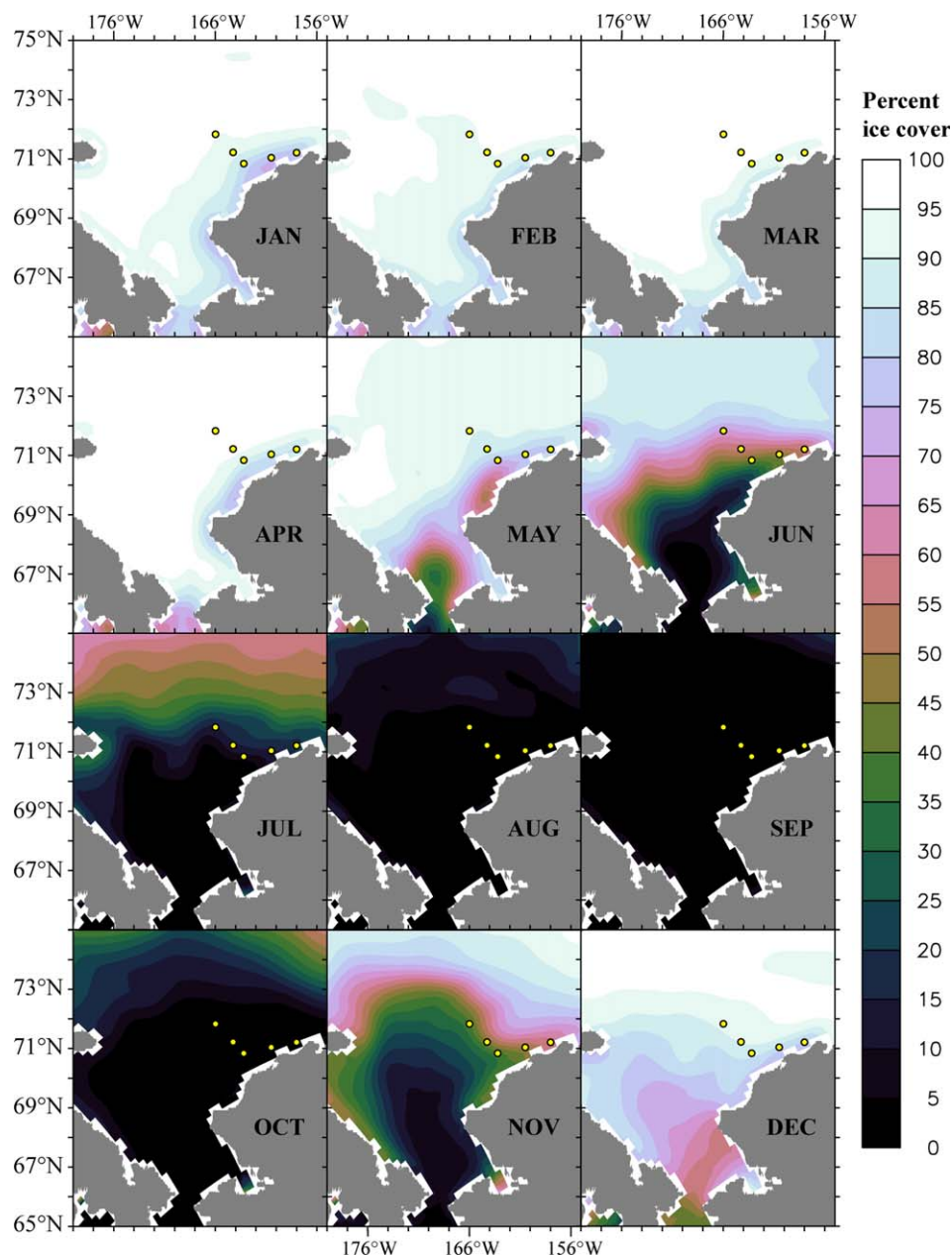


Figure 2. Monthly ice concentration climatology using SSM/I data from 2010/2011 winter to 2014/2015 winter.

Wind data from the NCEP North American Regional Reanalysis (NARR) interpolated to the location of mooring C2 (71.22°N, 164.25°W) were used to examine relationships between wind speed and direction and water properties observed at the moorings. The NARR data set was developed to provide higher spatial resolution and accuracy of temperatures and winds compared to available global reanalyses [Mesinger et al., 2006].

### 3. Results

#### 3.1. Sea Ice

Using monthly average ice concentration calculated from 2010 to 2015 (Figure 2), we describe the seasonal cycle of ice cover in the Chukchi Sea. From August to October, the Chukchi Sea is largely free of sea ice. Ice begins to advance from the north in October. Mean ice concentrations >30% are observed along the Siberian coastline south of Wrangel Island and along the eastern side of the Chukchi Sea in November/December.

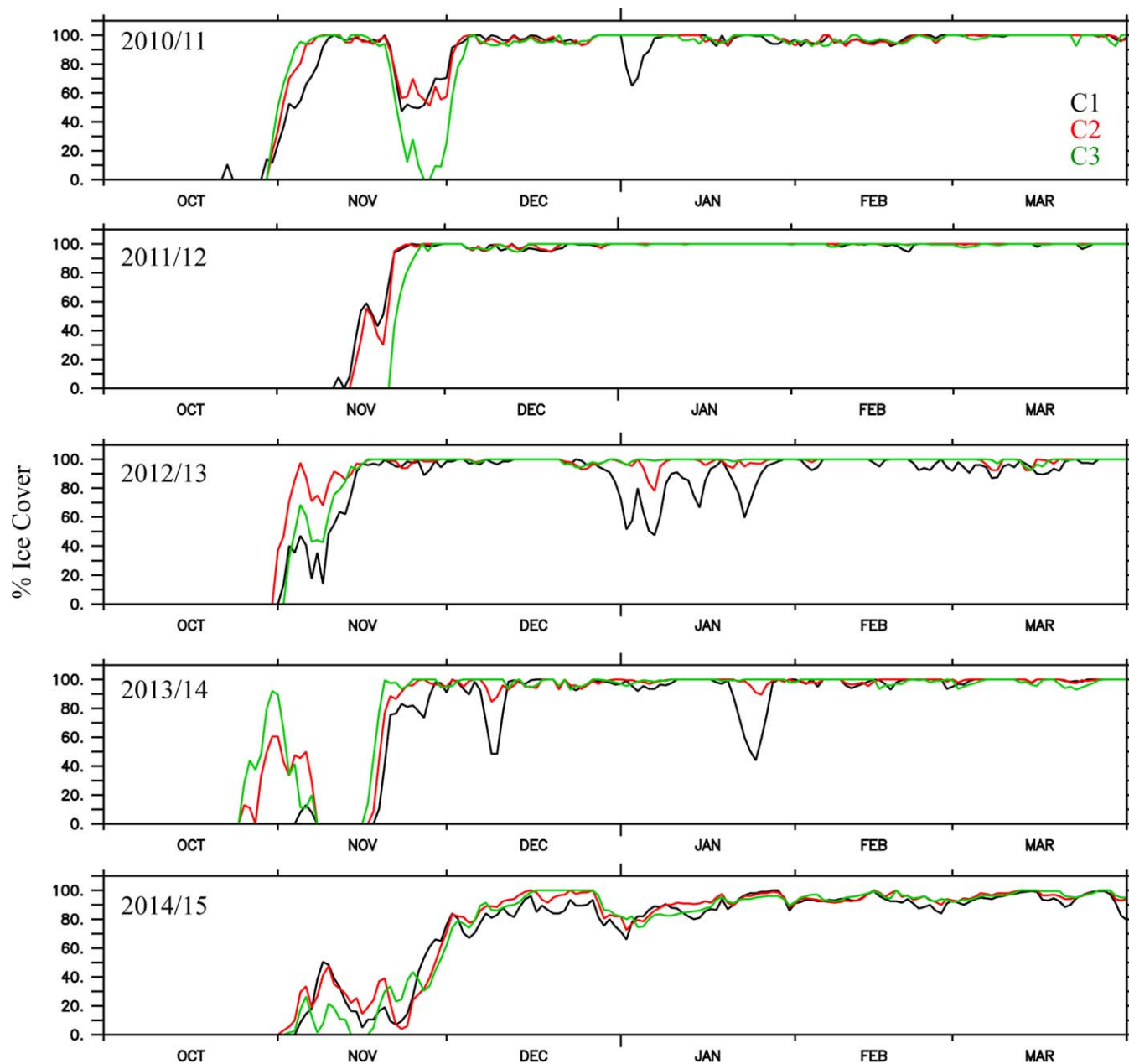


**Figure 3.** Daily average percent ice cover calculated from SSM/I data in the three regions surrounding moorings C1 (black), C2 (red), and C3 (green) during the five years of our study. See Figure 1 (red squares) for locations of the three regions.

From January to April, ice concentrations are  $>95\%$  throughout the Chukchi Sea except for the region along the Alaskan coast between Bering Strait and Point Barrow, where mean ice concentrations  $<85\%$  are observed in January. The Chukchi Polynya occurs in this region. Sea ice begins to retreat from the Chukchi Sea in May with earlier retreat in the polynya region along the Alaskan coast than similar latitudes elsewhere in the Chukchi Sea.

During the 5 years of our study, ice appears at our C1–C3 mooring locations in late October to mid-November and increases rapidly from 0% to  $\sim 100\%$  ice cover in a period of less than 2 weeks (Figure 3). After the initial ice advance, ice cover typically remains close to 100% until at least May, except during short-lived events (especially at C1, the mooring closest to the coast). These reduced ice cover events usually indicate the occurrence of the coastal polynya although occasionally, they are associated with a temporary retreat of the ice edge (i.e., late November 2010). During the 5 years of our study, polynyas occurred in

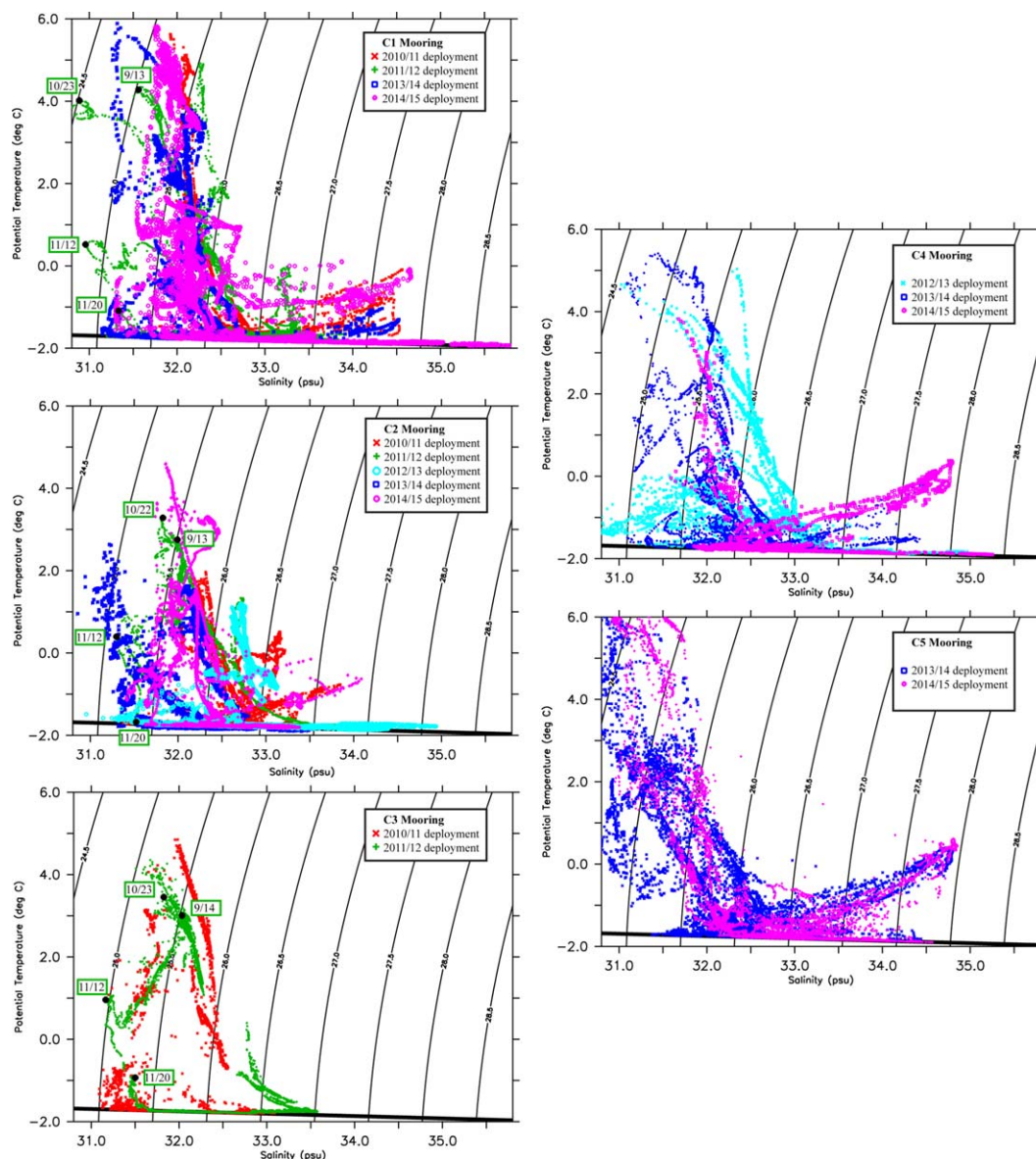


**Figure 4.** Potential temperature versus salinity plots for moorings (a) C1, (b) C2, (c) C3, (d) C4, and (e) C5. Data from each annual deployment are color coded: 2010/2011 (red), 2011/2012 (green), 2012/2013 (light blue), 2013/2014 (blue), and 2014/2015 (pink). Bold black line on each plot indicates freezing line. Dates of 2011/2012 warming/freshening events discussed in text are noted.

early January 2011, throughout January 2013, in mid-December 2013, and in late January 2014. The winter of 2011/2012 was notable for the lack of reduced ice cover while the winter of 2013/2014 exhibited much higher frequency of reduced ice cover events (Figure 3). In 2013/2014 and 2014/2015, reduced ice cover events were also more extensive spatially, impacting the regions around all three moorings.

### 3.2. Water Properties

The seasonal cycle of bottom waters on the eastern Chukchi Sea shelf generally trace a triangular pattern in temperature/salinity space (Figure 4) [see also Woodgate *et al.*, 2005b] with the vertices of the triangle denoted by the (1) warmest temperature, (2) lowest salinity, freezing temperature, and (3) higher salinity, freezing temperature. Each deployment of our moorings begins in August or September when the waters are generally warmest (near the top of the triangles). As autumn progresses, surface cooling and mixing (prior to the formation of ice) results in cooling and freshening of the bottom waters. As ice begins to form (typically in November), salinities begin to increase and temperatures are close to the freezing line. Over the

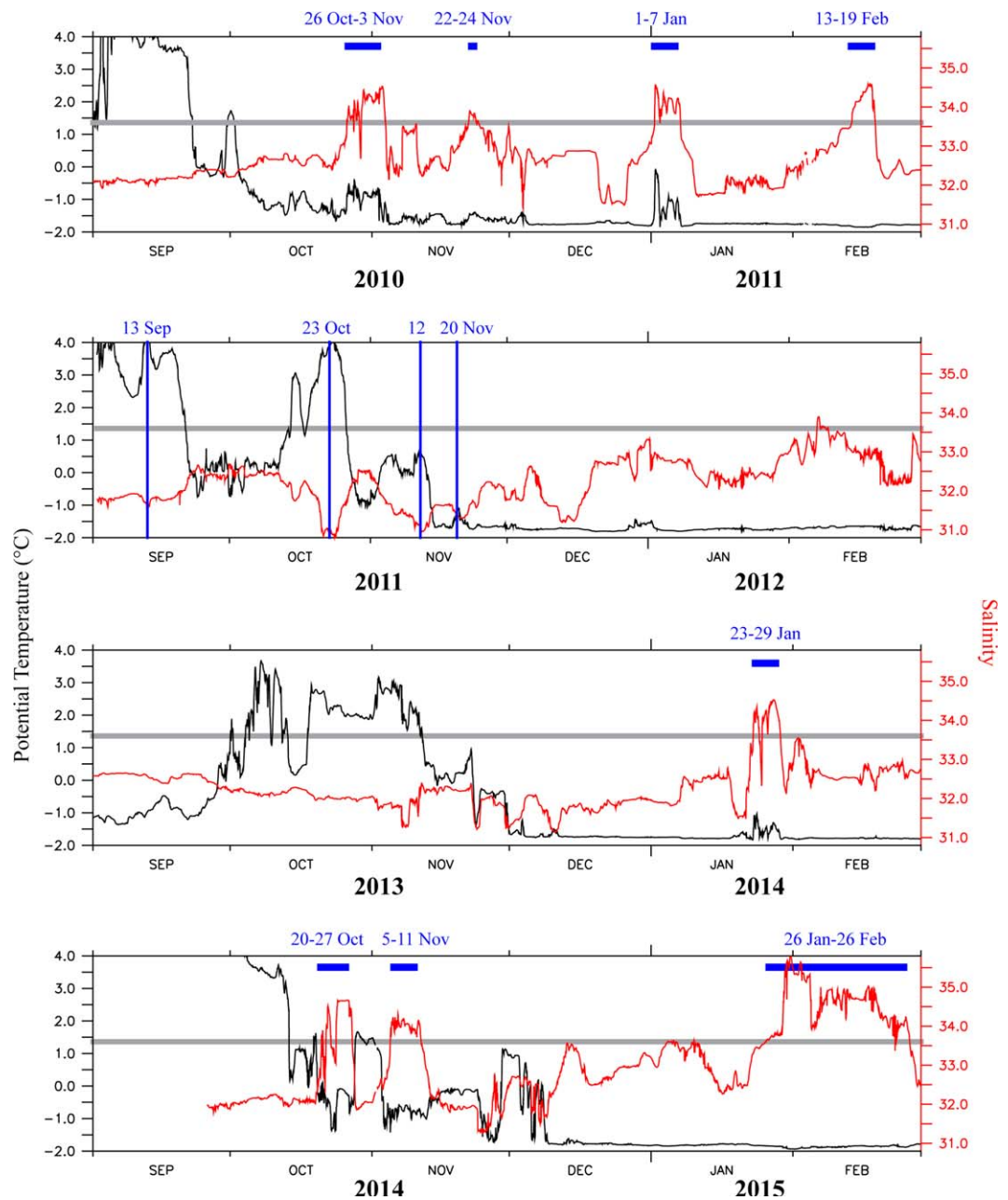


**Figure 5.** Potential temperature (black) and salinity (red) for each annual deployment of the C1 mooring. Horizontal gray line indicates salinity = 33.6. Periods when salinity >33.6 are indicated by blue bars. Periods in the fall of 2011 when temperature increased coincident with a decrease in salinity (discussed in text) are noted.

course of the winter, salinity varies from ~31.0 to over 34.0 depending on year and location, and temperatures mostly remain close to the freezing line. Finally, during spring and summer, the third leg of the triangle is completed with warming and freshening associated with surface heat fluxes and advection. This seasonal cycle in temperature and salinity is influenced both by local processes associated with ice formation/melt and convection/mixing, and by advection primarily from Bering Strait [Woodgate et al., 2005b].

The five moorings illustrate spatial differences in this triangular seasonal cycle. Of the three Icy Cape moorings (C1, C2, and C3), the warmest summer (August/September) waters are observed at C1 (>5°C) while C3 exhibits summer temperatures between 4 and 5°C. C2 exhibits the coldest summer temperatures (3–4°C in summer 2011 and 2014 but colder than 2°C in 2010 and 2012). This temperature difference is likely due to differences in vertical stratification among the three moorings.

**Table 2.** Events With  $S > 33.6$  at C1

Event	Dates	Duration (h)	Salinity		Temperature (°C)		Density ( $\sigma_{\theta}$ kg m <sup>-3</sup> )		Notes
			Ave	Max	Ave	Max	Ave	Max	
1	26 Oct to 3 Nov 2010	167	33.99	34.44	-0.8	-0.4	27.33	27.69	AW, ice advance
2	22–24 Nov 2010	49	33.76	33.90	-1.5	-1.4	27.16	27.28	AW influenced (too cold to be considered AW), ice edge
3	1–7 Jan 2011	126	34.11	34.56	-1.1	-0.1	27.43	27.76	AW, polynya
4	13–19 Feb 2011	125	34.23	34.59	-1.8	-1.8	27.56	27.85	Brine Rejection, 100% ice cover
5	23–29 Jan 2014	142	34.01	34.53	-1.5	-1.0	27.36	27.78	AW, polynya
6	20–27 Oct 2014	162	34.08	34.66	-0.5	0.1	27.39	27.85	AW, open water
7	5–11 Nov 2014	162	34.00	34.31	-0.8	-0.6	27.34	27.58	AW, ice edge
8	26 Jan to 26 Feb 2015	757	34.55	35.82	-1.9	-1.8	27.82	28.85	Brine Rejection, polynya

During winter, salinity  $>33.6$  was observed at C1 and C2, but not at C3. High salinities lying along the freezing line (Figure 4) indicate modification of PWW through brine rejection while salinity  $>33.6$  and temperature warmer than freezing indicate the presence (or at least influence) of upwelled Atlantic Water. Both brine rejection and AW are observed at C1 and C2. Upwelled AW is not observed at C3 (farthest from the coast). Moorings C4 and C5 (closer to Barrow Canyon) also show water properties consistent with upwelled AW in 2013/2014 and 2014/2015. Details of the AW upwelling events are discussed further below.

### 3.3. Atlantic Water Events

On the T/S plot (Figure 4), waters influenced by AW upwelling appear as a “tail” with high salinity and above-freezing temperatures on the right side of the plot. To examine the timing of these events, we plot time series of winter temperature and salinity at C1 and focus on events with  $S > 33.6$  (Figure 5). The time periods when  $S > 33.6$  in 2010, 2011, 2014, and 2015 are noted by blue bars at the top of the time series plots. No such events are observed at C1 in 2011/2012.

During autumn, temperature and salinity often vary inversely to each other. These events (e.g., 1 October 2010, 23 October 2011, 12 November 2011) oscillate between warmer/fresher ACW and cold/salty PWW. The 2011/2012 deployment clearly shows four separate events (see vertical blue lines and date labels in Figure 5) of warming/freshening with the peak of each event progressively cooler than the preceding events, presumably reflecting seasonal changes in the properties of the ACW. These events could be the result of local mixing, bringing surface ACW water properties to depth or advection of pulses of ACW past the mooring.

In contrast, the signature of AW intrusions is defined by events where salinity and temperature both increase together: salinity increases to  $>33.6$  and temperature increases above the freezing temperature. Out of the eight events noted by blue bars in Figure 5, six show this signature (Table 2). The events occurring on 13–19 February 2011 (event 4) and 26 January to 26 February 2015 (event 8) are different in that while  $S > 33.6$ ,  $T$  slightly decreases (staying right along the freezing line in Figure 4). This is a signature of brine rejection.

We will investigate the events shown in Table 2 in detail.

#### 3.3.1. Event 1: 26 October to 3 November 2010

On 26 October 2010, potential temperature abruptly increased from  $-1.3$  to  $-0.6^{\circ}\text{C}$  in less than a day (Figure 6). At the same time, salinity increased from 33.0 to 34.0. Temperature and salinity also increased at C2 (not shown) on 31 October (averaging  $-0.9^{\circ}\text{C}$ , 33.6 over 31 October to 3 November), indicating that the AW was relatively broadly distributed. C2 is approximately 55 km farther from the Alaskan coast than C1. While deep nitrate concentrations at C1 fluctuated between  $\sim 5$  and  $12 \mu\text{M/L}$  in the weeks prior to the event (Figure 6), nitrate was remarkably consistent during the event, averaging  $11.8 \mu\text{M/L}$  (0.5 standard deviation) indicating that the AW may be a significant source of nutrients to the Chukchi Shelf. Winds were strong ( $>10 \text{ m s}^{-1}$ ) and primarily out of the northeast for  $\sim 10$  days leading up to this event. Bottom currents were southwestward at speeds  $>20 \text{ cm s}^{-1}$  in the days leading up to the event.

In the 4–5 days prior to the event, the water column exhibited weak vertical shear except near the surface (Figure 6; bottom plot). With the onset of the event, shear increased dramatically suggesting active mixing throughout the water column. On 29 October, temperature, salinity, and nitrate concentrations abruptly but briefly decreased during high wind speeds ( $>15 \text{ m s}^{-1}$ ) suggesting the influence of mixing between the deep AW and

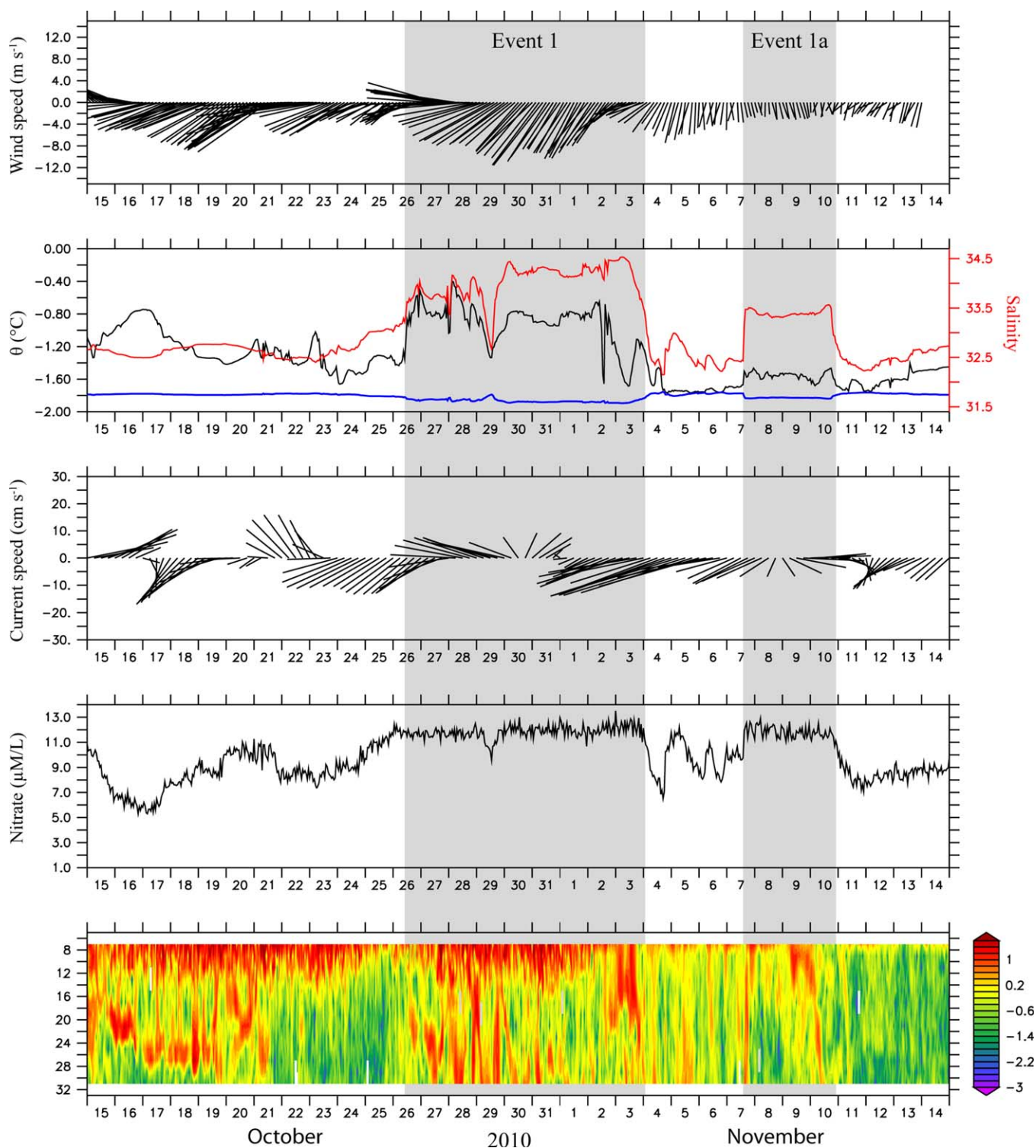


**Figure 6.** Time series of (a) NARR 10 m wind vectors (71.22°N, 164.25°W;  $m s^{-1}$ ); (b) potential temperature (black; °C), freezing temperature (blue; °C), and salinity (red); (c) current vectors ( $cm s^{-1}$ ); (d) nitrate ( $\mu M/L$ ); (e) Log of vertical shear squared. Except for NARR winds, all data were collected at C1. Events discussed in text are denoted by gray shading.

colder, fresher, nutrient-poor surface waters. A pulse of high shear descended from near the surface toward depth early on the 29th supporting the hypothesis of wind-induced mixing. After the mixing event, salinity and nitrate increased to previous levels. However, while temperature increased from the minimum ( $-1.3^{\circ}C$ ) observed on 29 October, it did not fully recover to the temperatures observed early in the event (averaging  $-0.8^{\circ}C$  during 26–28 October).

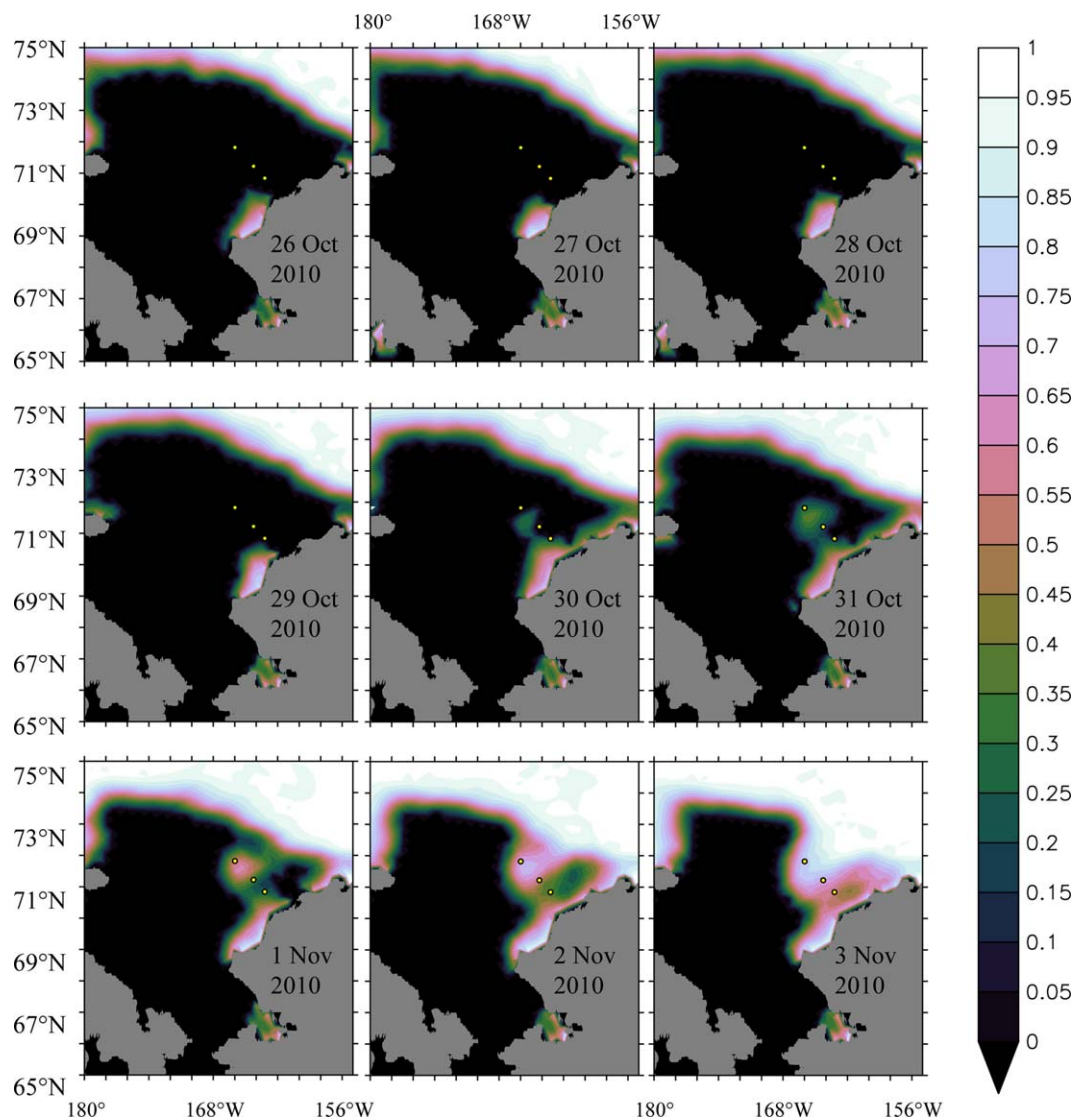


**Figure 7.** Daily SSM/I ice concentration from 26 October to 3 November 2010. Location of three moorings is denoted by yellow circles.

Elevated temperature and salinity at C1 continued until 3 November when temperature rapidly dropped to  $-1.7^{\circ}\text{C}$  (just  $0.2^{\circ}\text{C}$  above freezing) while salinity remained elevated at  $\sim 34.5$ , indicating the influence of brine rejection as ice began to close over the mooring. Ice concentration maps (Figure 7) suggest that ice formation was likely occurring during this time.

This entire event occurred during ice advance. At the beginning of the event, ice concentration at all three moorings was  $<10\%$  (Figures 3 and 7). By 30 October, ice concentration was nearing  $50\%$  near the coastline and concentrations at C1 were  $10\text{--}20\%$ . By 1 November, all three moorings were covered by  $>20\%$  ice concentration while a region of open water ( $<10\%$ ) remained northeast of the mooring line (closer to Barrow Canyon). We speculate that this pattern of ice advance (with more open water near the head of Barrow Canyon) is due to the influence of warm, upwelled AW delaying ice formation in the region.

Another weak event occurs on 7–10 November. This event shows a similar correspondence between increased temperature, salinity, and nitrate (event 1a; Figure 6). However, while temperatures warm above the freezing temperature indicating that this event is not due to brine rejection, the temperature signal is quite weak (an increase of  $\sim 0.2^{\circ}\text{C}$ ). Salinity approaches, but does not reach, the  $33.6$  threshold used for defining AW. This brief event may be a signature of upwelled AW that has mixed along the way and thus exhibits a much weaker signal.

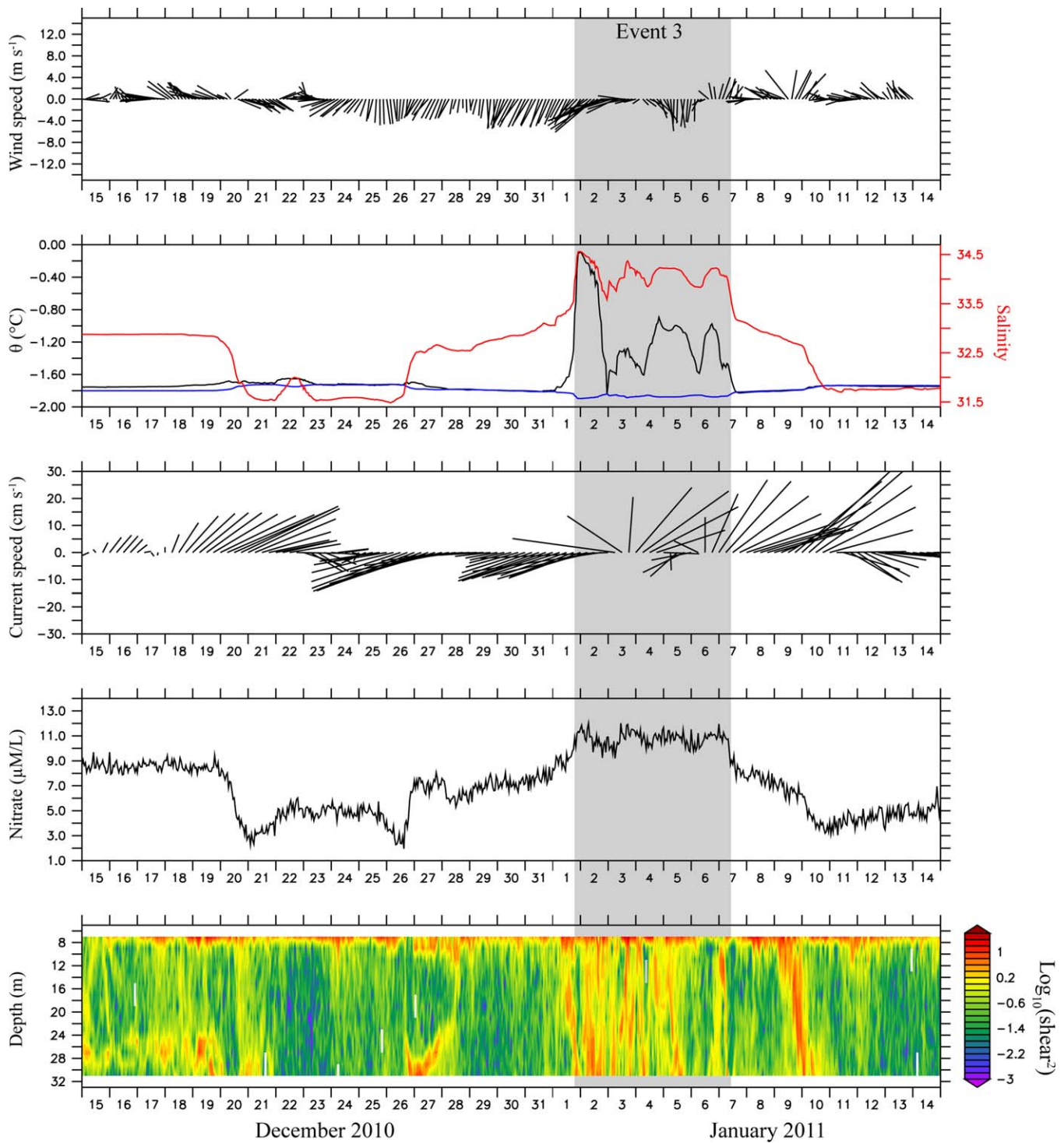


**Figure 8.** Time series of (a) NARR 10 m wind vectors (71.22°N, 164.25°W;  $m s^{-1}$ ); (b) potential temperature (black; °C), freezing temperature (blue; °C), and salinity (red); (c) current vectors ( $cm s^{-1}$ ); (d) nitrate ( $\mu M/L$ ); (e) log of vertical shear squared. Except for NARR winds, all data were collected at C1. Events discussed in text are denoted by gray shading.

### 3.3.2. Event 2: 22–24 November 2010

On 22 November 2010, salinity again increased to  $>33.6$  with an associated weak increase in temperature (Figure 5). This occurred during a retreat of the ice edge (not a polynya) that resulted in C3 being closer to the ice edge than the more coastal moorings C1 and C2 (Figure 3). The increase in salinity and temperature likely indicated another weak upwelling event but the temperature does not reach levels that would be considered AW.

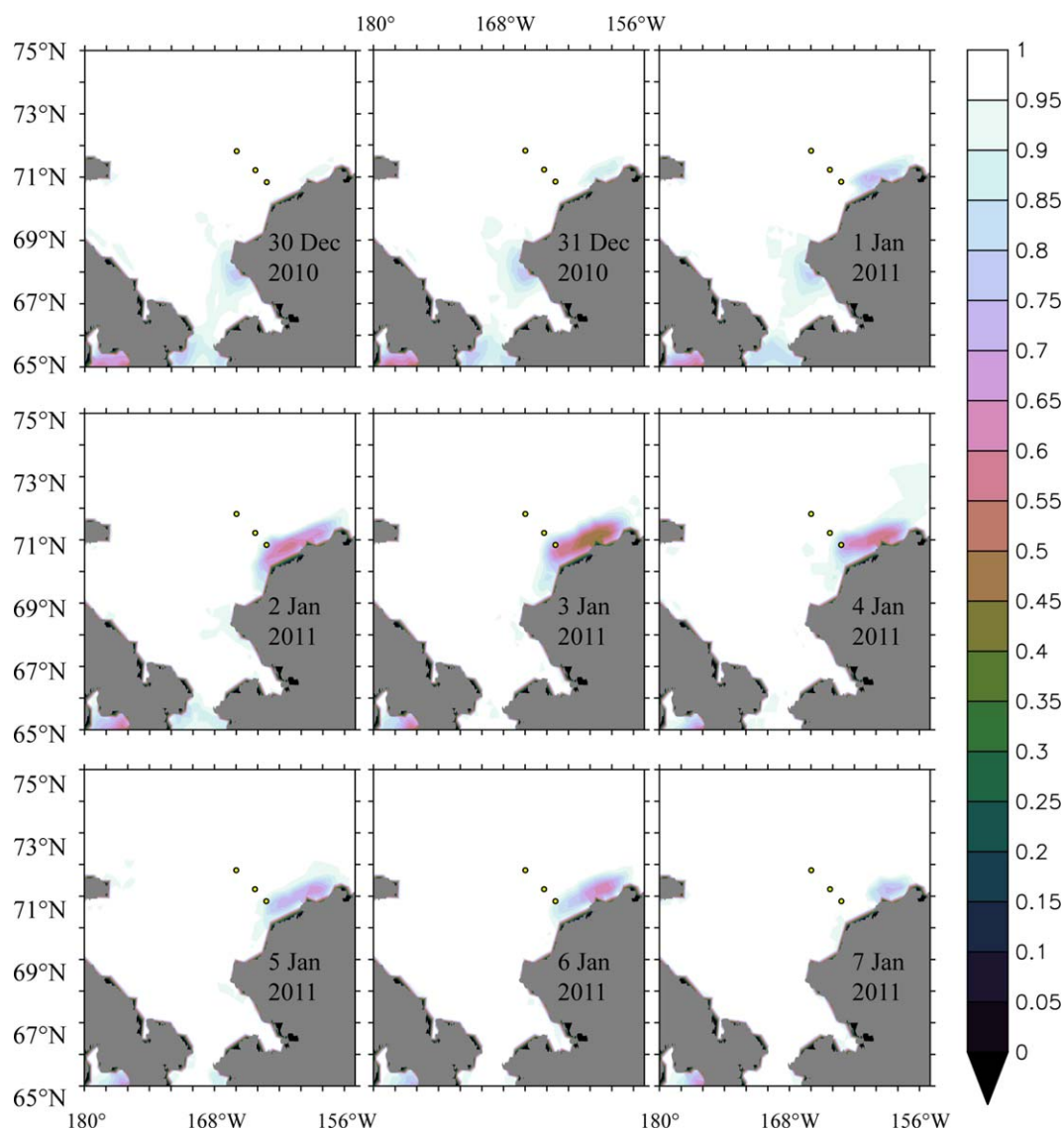


**Figure 9.** Daily SSM/I ice concentration from 30 December 2010 to 7 January 2011. Location of three moorings is denoted by yellow circles.

### 3.3.3. Event 3: 1–7 January 2011

Through most of December 2010, water temperature was very close to the freezing point (Figure 8) and ice cover over the mooring was close to 100% (Figure 3). On 1 January 2011, after  $\sim 10$  days of northerly winds, temperature at C1 increased from the freezing point ( $-1.8^{\circ}\text{C}$ ) to  $-0.1^{\circ}\text{C}$  in about 15 h (Figure 8). At the same time, salinity increased from 33.1 to 34.6 and nitrate concentration increased from 8.3 to 11.3  $\mu\text{M/L}$ . No sign of this event was observed at C2, indicating that the AW was tightly confined to the coast. The strongest temperature signal lasted only one day but temperatures remained mostly higher than freezing (and salinity and nitrate remained high) until 7 November. A brief dip to freezing temperature late on 2 January occurred while C1 was near the edge of the polynya (Figure 9) and may be a sign of brine rejection.

Ice concentration maps (Figure 9) show the development of a polynya at the same time AW is observed at C1. The polynya is first observed on 31 December 2010 northeast of the mooring line between Point Barrow and Wainwright. The region of reduced ice concentration moves southwestward over the next few days, reaching C1 on 2 January 2011. The lowest ice concentration values and largest horizontal extent occurs on 3 January before the polynya retreats back toward the northwest. However, even at its largest horizontal extent, the polynya does not appear to influence C2 (consistent with the lack of observed AW signal at C2). By 7 January, only a slight reduction in ice concentration is observed near Point Barrow.

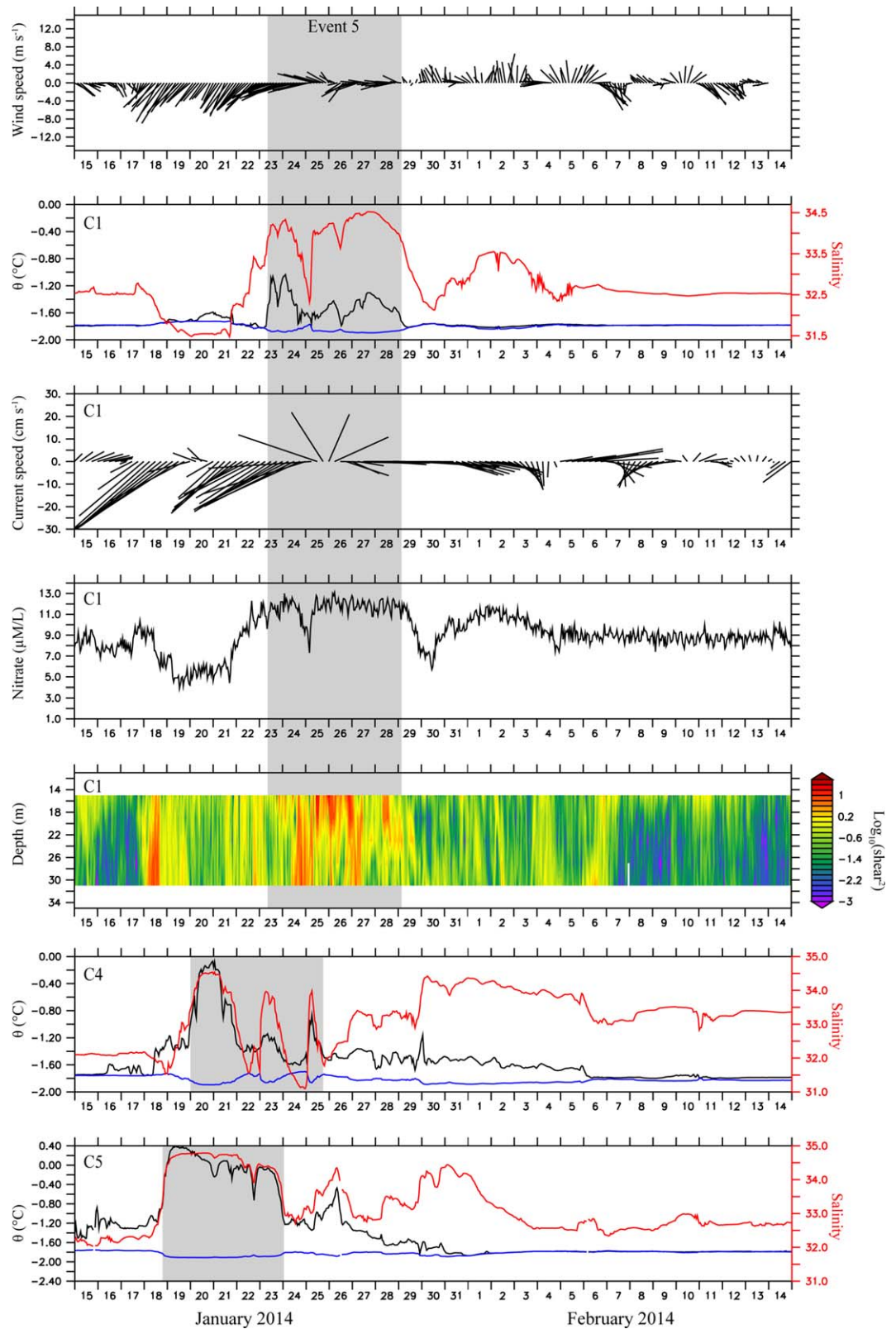


**Figure 10.** Time series of (a) NARR 10 m wind vectors (71.22°N, 164.25°W; m s<sup>-1</sup>); (b) potential temperature (black; °C), freezing temperature (blue; °C), and salinity (red); (c) current vectors (cm s<sup>-1</sup>); (d) nitrate (μM/L); (e) log of vertical shear squared; (f) potential temperature (black; °C), freezing temperature (blue; °C), and salinity (red) at C4; (g) potential temperature (black; °C), freezing temperature (blue; °C), and salinity (red) at C5. Events discussed in text are denoted by gray shading.

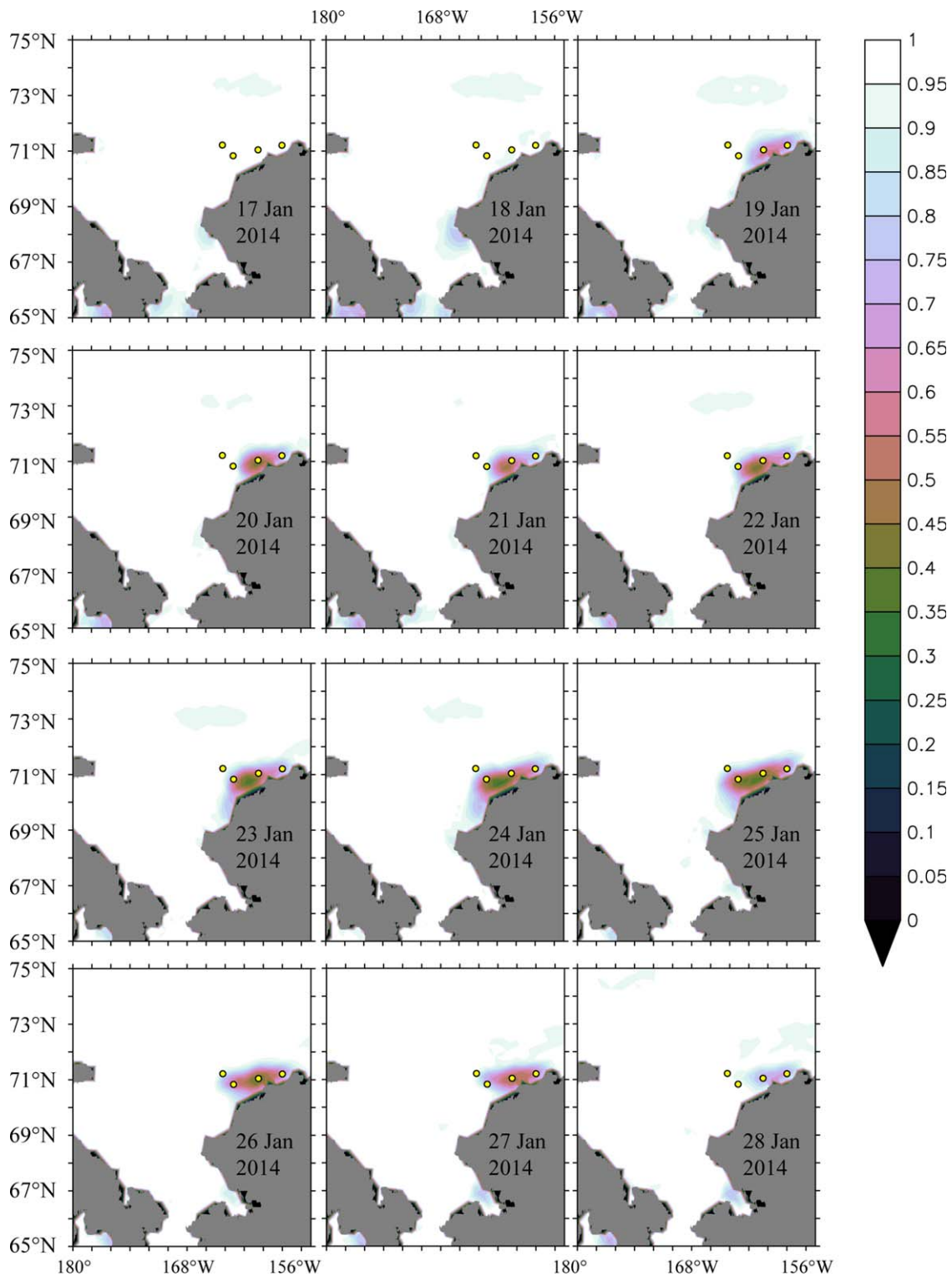
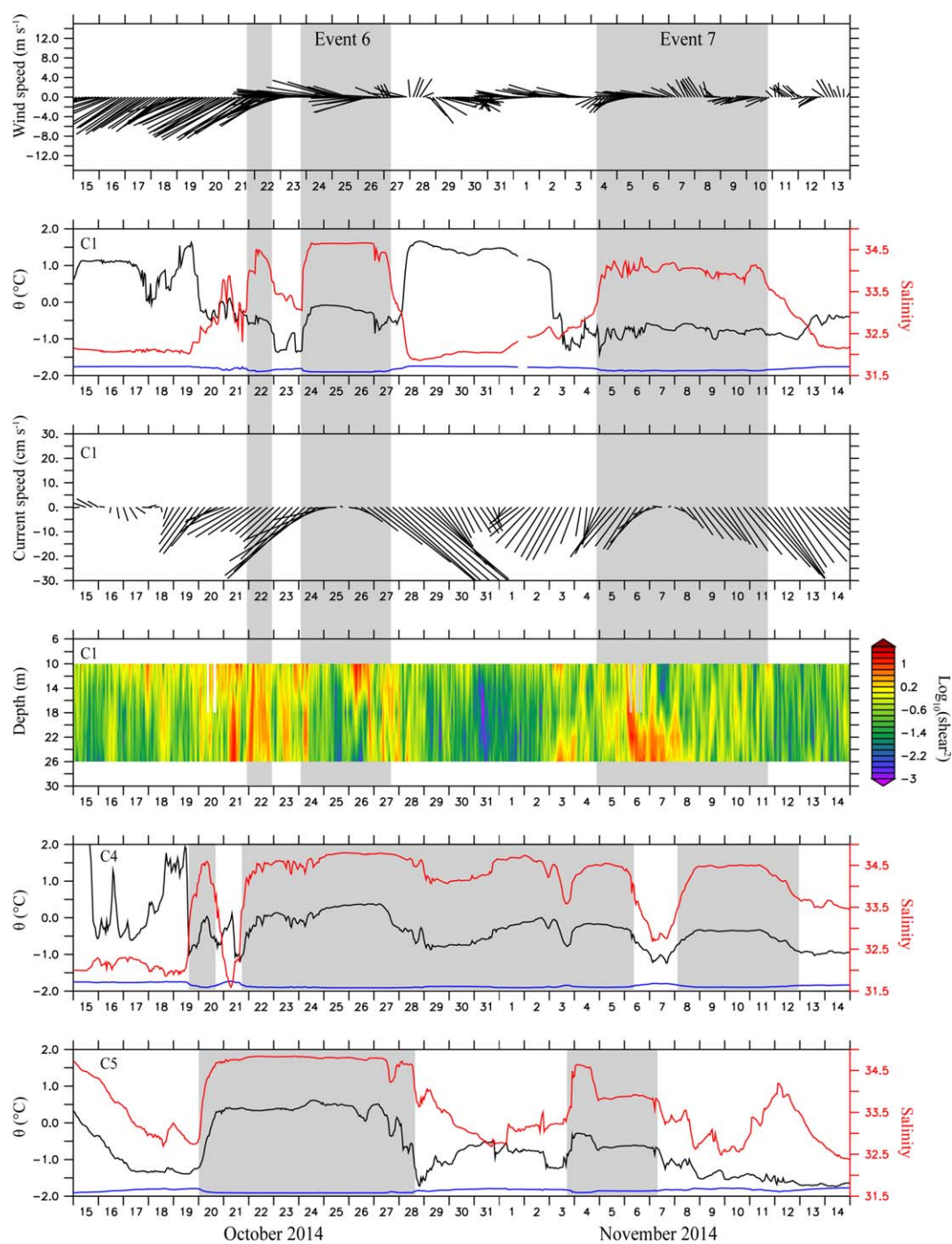


Figure 11. Daily SSM/I ice concentration from 17 January to 28 January 2014. Location of four moorings is denoted by yellow circles.

**3.3.4. Event 5: 23–29 January 2014**

At the C1 mooring, bottom salinity began increasing on 22 January 2014 with temperature beginning to increase approximately a day later (23 January 2014) (Figure 10). Temperature increased rapidly from  $-1.8$  to  $-1.1^{\circ}\text{C}$  in about 5 h. Nitrate concentrations also increased (averaging  $11.6 \mu\text{M}$  over 23–29 January)



**Figure 12.** Time series of (a) NARR 10 m wind vectors ( $71.22^{\circ}\text{N}$ ,  $164.25^{\circ}\text{W}$ ;  $\text{m s}^{-1}$ ); (b) potential temperature (black;  $^{\circ}\text{C}$ ), freezing temperature (blue;  $^{\circ}\text{C}$ ), and salinity (red); (c) current vectors ( $\text{cm s}^{-1}$ ); (d) log of vertical shear squared; (e) potential temperature (black;  $^{\circ}\text{C}$ ), freezing temperature (blue;  $^{\circ}\text{C}$ ), and salinity (red) at C4; (f) potential temperature (black;  $^{\circ}\text{C}$ ), freezing temperature (blue;  $^{\circ}\text{C}$ ), and salinity (red) at C5. Events discussed in text are denoted by gray shading.

coincident with the increased temperature and salinity. Salinity, temperature, and nitrate all decreased briefly on 25 January as winds turned to southerly and currents turned to northward. Temperatures remained above freezing until 29 January when winds changed from primarily easterly during the event to southerly.

The C4 mooring is approximately 100 km away from C1 and closer to Barrow Canyon (Figure 1). Increasing temperature and salinity were observed at C4 on 19–20 January, about 3 days earlier than at C1. An advective speed of  $\sim 40 \text{ cm s}^{-1}$  is required to travel 100 km in 3 days. In the period 19–23 January 2014, bottom

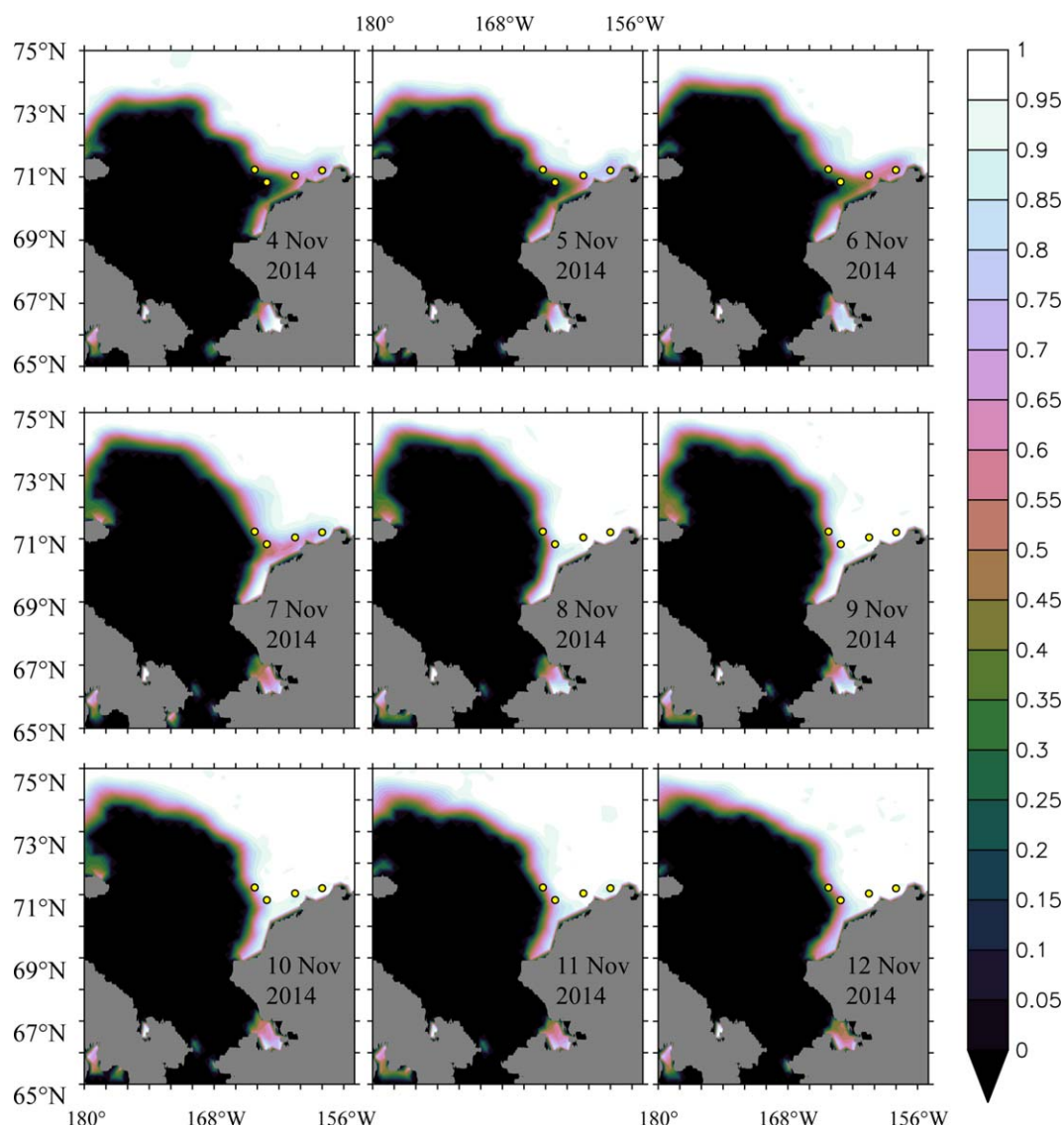


**Figure 13.** Daily SSM/I ice concentration (percent) from 4 November to 12 November 2014. Location of four moorings is denoted by yellow circles.

current speeds were southwestward at both C1 ( $32 \text{ cm s}^{-1}$ ) and C4 ( $48 \text{ cm s}^{-1}$ ), consistent with advection of the AW from C4 to C1. The C5 mooring deployed within Barrow Canyon also exhibited increased temperature and salinity with the signal appearing on 18 January. While temperatures fell to the freezing point at C1 on 29 January, they remained elevated at C4 (until 6 February) and C5 (until 1 February).

All four moorings (C1, C2, C4, and C5) were covered by 100% ice on 18 January 2014 (Figure 11). Coincident with the first appearance of increased temperature and salinity, the polynya first appeared on 19 January with reduced ice cover over C4 and C5 while C1 and C2 were still under 100% cover. The polynya advanced southwestward and by 22 January, C1 began to see reduced ice cover. The strongest polynya signal at C1 occurred around 24 January after which the polynya began to retreat back toward the northeast.

### 3.3.5. Event 6: 23–27 October 2014

Event 6 was unusual in that it occurred under open water conditions (Figure 3) prior to temperatures cooling to the freezing point (Figure 12). Salinity started to increase on 22 October after a period of strong northeasterly winds and southwestward bottom currents. High temperatures and salinities were also observed at C4 and C5 a couple days prior to the event at C1. High shear was observed at C1 on 21–24 October and 26–27 October suggesting active mixing. During 24–25 October, vertical shear was low,

currents were weak, and temperature and salinity were remarkably stable. The AW event ceased on 27 October with the arrival of warmer ( $>1^{\circ}\text{C}$ ), fresher ( $<32$ ) water coinciding with strong southeastward currents.

**3.3.6. Event 7: 5–11 November 2014**

Salinities began to increase on 5 November as C1 was under  $\sim 20\%$  ice cover at the edge of the advancing ice (Figures 12 and 13). Patterns of current flow were similar to event 6 with strong southwestward flow that weakened and rotated to the southeast over the course of the event. Both events 6 and 7 were preceded by AW passing the C5 mooring, and AW was evident almost continually from 19 October to 13 November at C4. Both of these events were observed at the C2 mooring as spikes in salinity and nitrate (not shown).

**3.3.7. Events 4 and 8: Brine Rejection Events**

On 13 February 2011, salinity at C1 rose above the 33.6 threshold, reaching a maximum of 34.6 on 17 February (Figure 5). At the same time, temperature was at the freezing point. This increase of salinity combined with freezing temperatures indicates water formed (or at least influenced) by brine rejection during ice formation. The Chukchi shelf was completely ice covered at the time (not shown) so it is unclear where the pulse of high salinity water came from. Currents were northeastward prior to the event suggesting that the water may have come from farther south although the ice edge was quite far away near the Bering Sea shelf-break at the time.

On 31 January 2015, salinity of 35.8 was observed at C1 (Figure 5), higher than previously recorded in 4 years of data at C1 (and to our knowledge higher than ever observed on the Chukchi Shelf). In addition to the Seacat measurement at 39 m, a SBE 37 microcat was also deployed nearby ( $<100$  m away) at 37 m. Both instruments recorded similar salinities, increasing confidence in the accuracy of these observations. These high salinities were associated with freezing temperatures, again indicating brine rejection. This event began under relatively weak ( $<10\text{ m s}^{-1}$ ) southerly winds and southeastward currents (not shown) although winds changed direction over the course of the event. The event coincided with a relatively extensive polynya that extended from Cape Lisburne to Icy Cape. This polynya did not follow the pattern of the other polynyas discussed in this paper (opening first near Barrow and advancing southward retreating back to north as it closed). In contrast, the polynya was strongest near Cape Lisburne and appeared to open and close in place. With no indication of upwelled AW, this polynya was likely a wind-driven polynya with no sensible heat mechanism operating. The brine rejection event observed in January/February 2015 at C1 may be quite rare as the other polynyas investigated here have been hybrid sensible heat/wind-driven polynyas exhibiting little brine rejection. In contrast to the AW events discussed above, high salinity was observed  $\sim 3$  days later at C4 suggesting northward advection.

**4. Discussion**

While Atlantic Water upwelling in Barrow Canyon has been found to exhibit high interannual variability [Aagaard and Roach, 1990; Weingartner et al., 1998], we have observed five AW events in four winters of data at C1, suggesting that AW regularly reaches farther onto the shelf than previously observed. These events typically occurred with northeasterly winds and southwestward currents with AW reaching the C1 mooring  $\sim 1$  week after the initiation of wind and current forcing. Wind and current direction combined with coincident observations closer to Barrow Canyon (C4, C5) suggest that the source of the AW observed at C1 is upwelling in Barrow Canyon.

Examining the ice cover (Figure 3) around the C1 mooring suggests that reductions in sea-ice concentration are often associated with upwelled AW. Unfortunately, no data were collected at C1 during January 2013 when ice cover was reduced over almost the entire month of January. While ice near the C2 mooring showed declines in January 2013, AW was not observed at C2. Within our 4 year observational record at C1, the only time that substantial ice reduction during winter was not accompanied by an AW signal was in mid-December 2013 (Figure 3).

**Table 3.** Heat Content of AW Events at C1 Relative to Freezing Temperature of  $-1.84^{\circ}\text{C}$  (Assuming 40 m Deep Water Column With Consistent Temperature)

AW Events	Heat Content	Thickness of Ice That can be Melted
Event 1 (26 Oct to 2 Nov 2010)	$1.66 \times 10^8\text{ J m}^{-2}$	0.5 m
Event 3 (1–7 Jan 2011)	$1.21 \times 10^8\text{ J m}^{-2}$	0.4 m
Event 5 (23–29 Jan 2014)	$0.54 \times 10^8\text{ J m}^{-2}$	0.2 m
Event 6 (20–27 Oct 2014)	$2.20 \times 10^8\text{ J m}^{-2}$	0.7 m
Event 7 (5–11 Nov 2014)	$1.70 \times 10^8\text{ J m}^{-2}$	0.5 m

Morales Maqueda *et al.* [2004] note that most shelf water polynyas are mechanically driven polynyas but there are exceptions. Many polynyas in the Canadian Arctic Archipelago are caused by surfacing of warm Atlantic Water (sensible heat mechanism) [Melling *et al.*, 2015]. In other cases, shelf water polynyas are maintained by a mixed sensible heat/wind-driven mechanism [Hirano *et al.*, 2016; Mysak and Huang, 1992]. Observations of vertical shear suggest that mixing from near bottom to near surface often occurs during the AW events suggesting that the observed warmer bottom temperatures could reach near the surface where they could influence the ice. Thus, it is possible that the warm upwelled AW observed at C1 could contribute to the opening and/or maintenance of the polynya in the eastern Chukchi Sea. However, it is difficult to tease apart the combined influence of the two mechanisms as easterly winds drive both a coastal divergence and upwelling at the shelf-break via Barrow Canyon [Hirano *et al.*, 2016]. Assuming the water column was well mixed and the temperature observed near the bottom at C1 was uniform throughout the water column, we can estimate the heat content of that column of water relative to freezing temperatures ( $T_f = -1.84^\circ\text{C}$  at  $S = 33.6$ ). Event 6 exhibited the highest heat content of the five AW events (Table 3). Assuming the heat content of the entire water column was available to melt ice, the heat content of event 6 was enough to melt  $\sim 0.7$  m thick ice. If that heat is continuously replenished over the lifetime of the event, ice melt due to sensible heat could act to delay ice formation and closing of the polynya. Thus, the observed AW events contain enough heat to have a significant influence on regional ice cover.

Coastal polynyas can be active areas of ice formation and enhanced brine rejection, resulting in hyper-saline varieties of PWW [Aagaard *et al.*, 1981; Weingartner *et al.*, 2005, 1998]. Ice formation depends on both the frequency of open water associated with the polynya and the temperature of the water within the polynya [Itoh *et al.*, 2012]. However, most heat budget estimates of brine rejection associated with the Chukchi Polynya have assumed that the water column temperature within the polynya was at the freezing point [e.g., Itoh *et al.*, 2012; Martin *et al.*, 2004; Weingartner *et al.*, 1998]. If the Chukchi Polynya is often influenced by the heat content of upwelled AW, then active ice formation would be reduced. At C1, during our 4 years of observations, brine rejection was infrequently observed, implying that the polynya may be less important to the production of high salinity PWW than previously assumed. Two instances of cold (freezing temperature), hyper-saline water were observed at C1. The first (event 4) occurred during 100% ice cover in the Chukchi Sea and was likely advected from farther south in the Bering Sea. The second (event 8), exhibited higher salinities than previously recorded on the Chukchi shelf and likely formed in a polynya near Cape Lisburne. Our time series at C1 suggest that polynyas north of Icy Cape are likely to be influenced by warm upwelled AW while polynyas observed farther south are more likely to be responsible for salinization of PWW.

Thinner ice may result in a longer partial ice season. Easterly winds produce the strongest upwelling response during the partial ice season [Schulze and Pickart, 2012]. Thus, the observed trend toward thinner ice in the Arctic [e.g., Lindsay *et al.*, 2009; Maslanik *et al.*, 2007] may result in enhanced effects of upwelling winds possibly resulting in more frequent and/or longer duration of events and larger spatial influence. If easterly winds can result in stronger upwelling of AW due to thinner ice, the influence of the sensible heat mechanism on polynya formation may be increasing.

#### Acknowledgments

Thanks to the captain, crews, and scientists aboard the *R/V Aquila* that deployed and recovered the moorings, particularly Catherine Berchok (chief scientist). Funding was provided by NOAA and the Bureau of Ocean Energy Management (BOEM) under Inter-Agency Agreements M09PG00016 (CHAOZ), M12PG00021 (ArcWEST), and M13PG00026 (CHAOZ-X). Special thanks to Carol Fairfield and Heather Crowley (BOEM) for their continued project support. This research is contribution EcoFOCI-0864 to NOAA's Fisheries-Oceanography Coordinated Investigations, contribution 4386 to NOAA's Pacific Marine Environmental Laboratory. This publication is partially funded by the Joint Institute for the Study of the Atmosphere and Ocean (JISAO) under NOAA Cooperative Agreement NA10OAR4320148, Contribution 2650. The mooring data are archived with the authors and BOEM and have been submitted to NOAA's National Centers for Environmental Information. The sea-ice data were downloaded from the National Snow and Ice Data Center (<http://nsidc.org/data/g02202>).

#### References

- Aagaard, K., and A. T. Roach (1990), Arctic ocean-shelf exchange: Measurements in Barrow Canyon, *J. Geophys. Res.*, *95*(C10), 18,163–18,175, doi:10.1029/JC095iC10p18163.
- Aagaard, K., L. K. Coachman, and E. Carmack (1981), On the halocline of the Arctic Ocean, *Deep Sea Res., Part A*, *28*(6), 529–545, doi:10.1016/0198-0149(81)90115-1.
- Bourke, R. H., and R. G. Paquette (1976), Atlantic water on the Chukchi Shelf, *Geophys. Res. Lett.*, *3*(10), 629–632, doi:10.1029/GL003i010p00629.
- Cavaliere, D. J., and S. Martin (1994), The contribution of Alaskan, Siberian, and Canadian coastal polynyas to the cold halocline layer of the Arctic-Ocean, *J. Geophys. Res.*, *99*(C9), 18,343–18,362, doi:10.1029/94JC01169.
- Cavaliere, D. J., P. Gloersen, and W. J. Campbell (1984), Determination of sea ice parameters with the NIMBUS-7 SMMR, *J. Geophys. Res.*, *89*(D4), 5355–5369, doi:10.1029/JD089iD04p05355.
- Coachman, L. K., and K. Aagaard (1966), On the water exchange through Bering Strait, *Limnol. Oceanogr.*, *11*(1), 44–59, doi:10.4319/lo.1966.11.1.0044.
- Coachman, L. K., K. Aagaard, and R. B. Tripp (1975), *Bering Strait: The Regional Physical oceanography*, Univ. of Washington Press, Seattle, Wash.
- Comiso, J. C. (1986), Characteristics of Arctic winter sea ice from satellite multispectral microwave observations, *J. Geophys. Res.*, *91*(C1), 975–994, doi:10.1029/JC091iC01p00975.
- Danielson, S. L., L. Eisner, C. Ladd, C. Mordy, L. Sousa, and T. J. Weingartner (2016), A comparison between late summer 2012 and 2013 water masses, macronutrients, and phytoplankton standing crops in the northern Bering and Chukchi Seas, *Deep Sea Res., Part II*, doi:10.1016/j.dsr2.2016.05.024.

- Garrison, G. R., and R. G. Paquette (1982), Warm water interactions in the Barrow Canyon in winter, *J. Geophys. Res.*, *87*(C8), 5853–5859, doi:10.1029/JC087iC08p05853.
- Gong, D., and R. S. Pickart (2015), Summertime circulation in the eastern Chukchi Sea, *Deep Sea Res., Part II*, *118*, 18–31, doi:10.1016/j.dsr2.2015.02.006.
- Hirano, D., Y. Fukamachi, E. Watanabe, K. I. Ohshima, K. Iwamoto, A. R. Mahoney, H. Eicken, D. Simizu, and T. Tamura (2016), A wind-driven, hybrid latent and sensible heat coastal polynya off Barrow, Alaska, *J. Geophys. Res. Oceans*, *121*, 980–997, doi:10.1002/2015JC011318.
- Itoh, M., K. Shimada, T. Kamoshida, F. McLaughlin, E. Carmack, and S. Nishino (2012), Interannual variability of Pacific Winter Water inflow through Barrow Canyon from 2000 to 2006, *J. Oceanogr.*, *68*(4), 575–592, doi:10.1007/s10872-012-0120-1.
- Itoh, M., S. Nishino, Y. Kawaguchi, and T. Kikuchi (2013), Barrow Canyon volume, heat, and freshwater fluxes revealed by long-term mooring observations between 2000 and 2008, *J. Geophys. Res. Oceans*, *118*, 4363–4379, doi:10.1002/jgrc.20290.
- Kozo, T. L. (1991), The hybrid polynya at the northern end of Nares Strait, *Geophys. Res. Lett.*, *18*(11), 2059–2062, doi:10.1029/91GL02574.
- Lindsay, R. W., J. Zhang, A. Schweiger, M. Steele, and H. Stern (2009), Arctic Sea Ice retreat in 2007 follows thinning trend, *J. Clim.*, *22*(1), 165–176, doi:10.1175/2008JCLI2521.1.
- Martin, S., R. Drucker, R. Kwok, and B. Holt (2004), Estimation of the thin ice thickness and heat flux for the Chukchi Sea Alaskan coast polynya from Special Sensor Microwave/Imager data, 1990–2001, *J. Geophys. Res.*, *109*, C10012, doi:10.1029/2004JC002428.
- Maslanik, J. A., C. Fowler, J. Stroeve, S. Drobot, J. Zwally, D. Yi, and W. Emery (2007), A younger, thinner Arctic ice cover: Increased potential for rapid, extensive sea-ice loss, *Geophys. Res. Lett.*, *34*, L24501, doi:10.1029/2007GL032043.
- Meier, W., F. Fetterer, M. Savoie, S. Mallory, R. Duerr, and J. Stroeve (2013, updated 2015), *NOAA/NSIDC Climate Data Record of Passive Microwave Sea Ice Concentration*, Version 2, Natl. Snow and Ice Data Cent., Boulder, Colo., doi:10.7265/N55M63M1.
- Melling, H., R. A. Lake, D. R. Topham, and D. B. Fissel (1984), Oceanic thermal structure in the western Canadian Arctic, *Cont. Shelf Res.*, *3*(3), 233–258, doi:10.1016/0278-4343(84)90010-4.
- Melling, H., C. Haas, and E. Brossier (2015), Invisible polynyas: Modulation of fast ice thickness by ocean heat flux on the Canadian polar shelf, *J. Geophys. Res. Oceans*, *120*, 777–795, doi:10.1002/2014JC010404.
- Mesinger, F., et al. (2006), North American regional reanalysis, *Bull. Am. Meteorol. Soc.*, *87*(3), 343–360, doi:10.1175/bams-87-3-343.
- Morales Maqueda, M. A., A. J. Willmott, and N. R. T. Biggs (2004), Polynya dynamics: A review of observations and modeling, *Rev. Geophys.*, *42*, RG1004, doi:10.1029/2002RG000116.
- Mountain, D. G., L. K. Coachman, and K. Aagaard (1976), On the flow through Barrow Canyon, *J. Phys. Oceanogr.*, *6*(4), 461–470, doi:10.1175/1520-0485(1976)006<0461:OTFTBC>2.0.CO;2.
- Mysak, L. A., and F. Huang (1992), A Latent-and Sensible-Heat Polynya Model for the North Water, Northern Baffin Bay, *J. Phys. Oceanogr.*, *22*(6), 596–608, doi:10.1175/1520-0485(1992)022<0596:ALASHP>2.0.CO;2.
- Peng, G., W. N. Meier, D. J. Scott, and M. H. Savoie (2013), A long-term and reproducible passive microwave sea ice concentration data record for climate studies and monitoring, *Earth Syst. Sci. Data*, *5*(2), 311–318, doi:10.5194/essd-5-311-2013.
- Pickart, R. S., G. W. K. Moore, D. J. Torres, P. S. Fratantoni, R. A. Goldsmith, and J. Y. Yang (2009), Upwelling on the continental slope of the Alaskan Beaufort Sea: Storms, ice, and oceanographic response, *J. Geophys. Res.*, *114*, C00A13, doi:10.1029/2008JC005009.
- Pickart, R. S., L. J. Pratt, D. J. Torres, T. E. Whitledge, A. Y. Proshutinsky, K. Aagaard, T. A. Agnew, G. W. K. Moore, and H. J. Dail (2010), Evolution and dynamics of the flow through Herald Canyon in the western Chukchi Sea, *Deep Sea Res., Part II*, *57*(1–2), 5–26, doi:10.1016/j.dsr2.2009.08.002.
- Pickart, R. S., M. A. Spall, G. W. K. Moore, T. J. Weingartner, R. A. Woodgate, K. Aagaard, and K. Shimada (2011), Upwelling in the Alaskan Beaufort Sea: Atmospheric forcing and local versus non-local response, *Prog. Oceanogr.*, *58*(1–4), 78–100, doi:10.1016/j.pocean.2010.11.005.
- Pickart, R. S., M. A. Spall, and J. T. Mathis (2013), Dynamics of upwelling in the Alaskan Beaufort Sea and associated shelf-basin fluxes, *Deep Sea Res., Part I*, *76*, 35–51, doi:10.1016/j.dsr.2013.01.007.
- Schulze, L. M., and R. S. Pickart (2012), Seasonal variation of upwelling in the Alaskan Beaufort Sea: Impact of sea ice cover, *J. Geophys. Res.*, *117*, C06022, doi:10.1029/2012JC007985.
- Shimada, K., M. Itoh, S. Nishino, F. McLaughlin, E. Carmack, and A. Proshutinsky (2005), Halocline structure in the Canada basin of the arctic ocean, *Geophys. Res. Lett.*, *32*, L03605, doi:10.1029/2004GL021358.
- Weingartner, T. J., D. J. Cavalieri, K. Aagaard, and Y. Sasaki (1998), Circulation, dense water formation, and outflow on the northeast Chukchi shelf, *J. Geophys. Res.*, *103*(C4), 7647–7661, doi:10.1029/98JC00374.
- Weingartner, T., K. Aagaard, R. Woodgate, S. Danielson, Y. Sasaki, and D. Cavalieri (2005), Circulation on the north central Chukchi Sea shelf, *Deep Sea Res., Part II*, *52*(24–26), 3150–3174, doi:10.1016/j.dsr2.2005.10.015.
- Williams, W. J., E. C. Carmack, K. Shimada, H. Melling, K. Aagaard, R. W. Macdonald, and R. G. Ingram (2006), Joint effects of wind and ice motion in forcing upwelling in Mackenzie Trough, Beaufort Sea, *Cont. Shelf Res.*, *26*(19), 2352–2366, doi:10.1016/j.csr.2006.06.012.
- Woodgate, R. A., and K. Aagaard (2005), Revising the Bering Strait freshwater flux into the Arctic Ocean, *Geophys. Res. Lett.*, *32*, L02602, doi:10.1029/2004GL021747.
- Woodgate, R. A., K. Aagaard, and T. J. Weingartner (2005a), Monthly temperature, salinity, and transport variability of the Bering Strait through flow, *Geophys. Res. Lett.*, *32*, L04601, doi:10.1029/2004GL021880.
- Woodgate, R. A., K. Aagaard, and T. J. Weingartner (2005b), A year in the physical oceanography of the Chukchi Sea: Moored measurements from autumn 1990–1991, *Deep Sea Res., Part II*, *52*(24–26), 3116–3149, doi:10.1016/j.dsr2.2005.10.016.